

Covariate Gaussian Process Latent Variable Models

Kaspar Märtens¹, Kieran R Campbell^{2,3}, and Christopher Yau^{4,5}

¹Department of Statistics, University of Oxford, Oxford, United Kingdom

²Department of Statistics, University of British Columbia, Vancouver BC, Canada

³UBC Data Science Institute, University of British Columbia, Vancouver BC, Canada

⁴Institute of Cancer and Genomic Sciences, University of Birmingham, United Kingdom

⁵Alan Turing Institute, London, United Kingdom

Abstract

Gaussian Process Regression (GPR) and Gaussian Process Latent Variable Models (GPLVM) offer a principled way of performing probabilistic non-linear regression and dimensionality reduction. In this paper we propose a hybrid between the two, the covariate-GPLVM (c-GPLVM), to perform dimensionality reduction in the presence of covariate information (e.g. continuous covariates, class labels, or censored survival). This construction lets us adjust for covariate effects and reveals meaningful latent structure which is not revealed when using GPLVM. Furthermore, we introduce structured decomposable kernels which will let us interpret how the fixed and latent inputs contribute to feature-level variation, e.g. identify the presence of a non-linear interaction. We demonstrate the utility of this model on applications in disease progression modelling from high-dimensional gene expression data in the presence of additional phenotypes.

1 Introduction

The identification of low-dimensional structure is crucial to gaining insight from complex high-dimensional data. In probabilistic models, this task can be formulated as finding a low-dimensional latent variable $\mathbf{z}_n \in \mathbb{R}^Q$ for each data point $n = 1, \dots, N$ and a set of mappings $f^{(j)} : \mathbf{z} \mapsto \mathbf{y}^{(j)}$ for every feature $\mathbf{y}^{(j)}$, $j \in \{1, \dots, P\}$ so that $Q \ll P$. Obtaining an informative one- or two-dimensional representation of the data is often particularly desirable, allowing us to visually interpret the patterns and relationships present in the data such demands have driven the increased use of t-SNE [Maaten and Hinton, 2008] for instance.

There are a number of approaches for defining the mapping functions ranging from linear models [Tipping and Bishop, 1999] to non-linear models provided by neural networks [Kingma and Welling, 2014, Sønderby et al., 2016, Kusner et al., 2017]. In this work we particularly focus on the use of Gaussian Processes (GP) as a non-parametric model over the mapping functions, i.e. the GP Latent Variable Model (GPLVM) [Lawrence, 2005]. Our choice reflects the strong theoretical underpinnings of GP models as well as recent advances that have enabled such models to be scalable to large data sets [Hensman et al., 2013, 2015b].

In particular, we focus on the scenario where, in addition to $(\mathbf{z}_n, \mathbf{y}_n)$, each data point is also associated with a C -dimensional covariate vector, $\mathbf{x}_n \in \mathbb{R}^C$. This is motivated by an observation that real-life data often exhibits strong structure which is *a priori* known to us, i.e. there is a small number of covariates (such as continuous-valued measurements, class labels, or censored survival times) which might act to modulate the variation in the data.

Figure 1 illustrates our setting of interest where feature values vary over the latent coordinate and over the covariate (which could be continuous or discrete). This dependence on the covariate might confound the

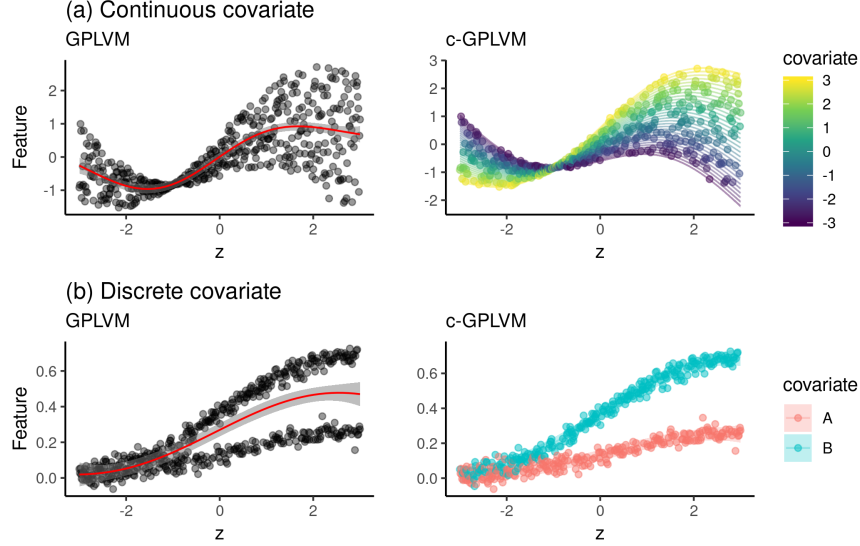


Figure 1: The presence of covariate effects confounds the mappings from the underlying latent \mathbf{z} (on x -axis) to the feature space (y -axis). This has been illustrated for (a) a continuous covariate, and (b) a categorical one. A standard GPLVM necessarily ignores covariate information, whereas its inclusion in c-GPLVM allows it to capture a variety of nonlinear covariate effects.

mappings from \mathbf{z} to $\mathbf{y}^{(j)}$ when applying a standard latent variable model, such as GPLVM, which would fail to account for the underlying latent structure in the data that is shared across all covariate values. In principle, covariate effects can be incorporated in the model in various ways (e.g. graphical models in Figure 2). Our proposal, which we call the *covariate-GPLVM* (c-GPLVM), specifically focuses on learning a set of mappings $f^{(j)} : (\mathbf{z}, \mathbf{x}) \mapsto \mathbf{y}^{(j)}$ which are defined on the joint space of \mathbf{z} and \mathbf{x} . This can be seen as a hybrid between the GP regression and the GP latent variable model where the input space consists of two parts: fixed covariates \mathbf{x} and unobserved latent coordinates \mathbf{z} (in contrast, in the former the inputs are fixed, whereas in the latter the inputs are random variables and they are inferred). This construction lets us additionally handle partially missing or censored covariates. The goal of our work is specifically to *adjust* for covariate effects when forming the latent space.

The concept of a *covariate-adjusted* latent space \mathbf{z} is illustrated in Figure 3. Here, we use GPLVM, supervised-GPLVM and c-GPLVM to learn a 2-D latent space from the same synthetic data set which contains 5 discrete classes (A-E). The dominant effect of these classes means a GPLVM will learn a latent space that reflects the presence of these groups. This is further exaggerated with the supervised-GPLVM which acts to increase the separation between the classes and is most useful if class discrimination is the ultimate objective. In contrast, the c-GPLVM seeks to find the common shared structure between the 5 classes, and computes an inferred latent space which adjusts for the presence of the 5 classes (in linear modelling this process would be analogous to “regressing out” the class-specific effects). If the five different classes corresponded to five subtypes of a particular disease, (supervised)-GPLVM would find a latent space that would enable a low-dimensional characterisation of the five subtypes but c-GPLVM seeks to find what aspects of these five subtypes are common.

Furthermore, we are particularly interested in mappings that enable a variance decomposition of the observed data into components which are driven by (i) the fixed inputs only, (ii) the latent inputs, and (iii) variation that is driven by some non-linear interaction between the fixed and latent inputs. To achieve this, we construct a structured kernel decomposition which will let us explicitly capture these three types of interactions, informing us whether an additive model is sufficient to explain the covariate effects or if there exist additional interactions.

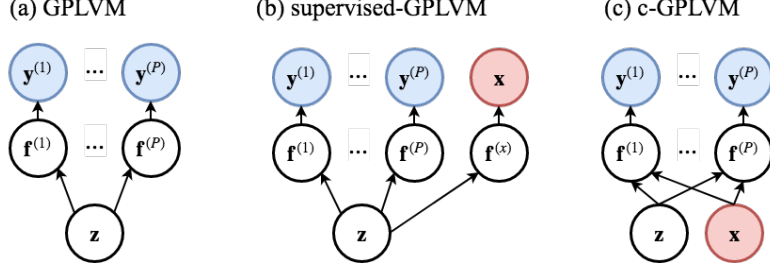


Figure 2: Graphical models for (a) GPLVM, (b) a particular implementation of supervised-GPLVM, and (c) c-GPLVM.

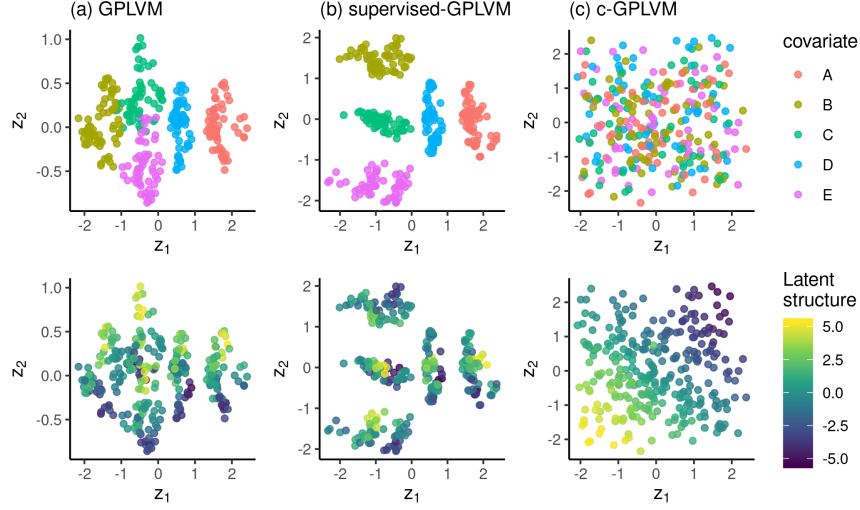


Figure 3: The latent \mathbf{z} inferred by c-GPLVM differs fundamentally from what is inferred by GPLVM and supervised-GPLVM. For all three methods, their learned 2D latent space \mathbf{z} has been shown twice, coloured according to the categorical covariate (top panel) and the underlying latent structure (bottom panel). In the presence of both between-cluster effects (highlighted in top row) and shared within-cluster latent structure (bottom row), the \mathbf{z} inferred by GPLVM reflects the former but not the latter. This effect is even stronger for supervised-GPLVM which encourages \mathbf{z} to *discriminate* between the clusters. Instead, c-GPLVM will *adjust* for the cluster effects and thus reveal the latent structure which is *shared* between all clusters.

The latter makes c-GPLVM especially appealing for non-linear modelling in real-world applications such as disease progression modelling.

2 Background on Gaussian Processes

2.1 Gaussian Process regression

Gaussian processes offer a principled non-parametric framework for inference over functions [Rasmussen and Williams, 2006]. Consider a real valued function defined on the D -dimensional inputs $\mathbf{X} := (\mathbf{x}_1, \dots, \mathbf{x}_N)$. A function f is said to be drawn from a GP with mean $\mathbf{0}$ and covariance $k(\mathbf{x}, \mathbf{x}')$, denoted by $f(\mathbf{x}) \sim$

$\mathcal{GP}(\mathbf{0}, k(\mathbf{x}, \mathbf{x}'))$, when

$$p(\mathbf{f}|\mathbf{X}, \theta) = \mathcal{N}(\mathbf{f}|\mathbf{0}, \mathbf{K})$$

where \mathbf{K} is the kernel matrix of all pairs of inputs which also depends on hyperparameters θ , with elements $\mathbf{K}_{ij} := k(\mathbf{x}_i, \mathbf{x}_j)$. One popular choice for $k(\cdot)$ is the squared exponential ARD kernel,

$$k(\mathbf{x}_i, \mathbf{x}_k) = \sigma_{\square}^2 \left(-\frac{1}{2} \sum_{j=1}^D \frac{(x_{ij} - x_{kj})^2}{l_j^2} \right)$$

where σ_{\square}^2 is the kernel variance parameter and l_j are the feature-specific lengthscales. Combining the GP prior with a given likelihood $p(\mathbf{y}|\mathbf{f})$ can lead to a variety of models, e.g. the GP regression model (for the Gaussian likelihood) or the GP classification model (for the categorical softmax distribution).

2.2 Gaussian Process Latent Variable Model

GPLVM is a latent variable model which uses GPs as latent mappings, being a non-linear extension of the probabilistic PCA [Lawrence, 2005]. Suppose we have an observed data matrix \mathbf{Y} , consisting of P features $(\mathbf{y}^{(1)}, \dots, \mathbf{y}^{(P)})$ and N data points, and our goal is to learn a low-dimensional representation $\mathbf{Z} := (\mathbf{z}_1, \dots, \mathbf{z}_N)$. When conditioning on the latent variable \mathbf{z} , the GPLVM is essentially a multi-output GP regression model as it specifies a GP prior for every latent mapping $\mathbf{f}^{(j)}$ and some likelihood $p(\mathbf{y}^{(j)}|\mathbf{f}^{(j)})$ for $j \in \{1, \dots, P\}$. Placing a prior over the low-dimensional \mathbf{z} our aim is to infer the respective posterior. Denoting the collection of GP function values $\mathbf{F} := (\mathbf{f}^{(1)}, \dots, \mathbf{f}^{(P)})$, the GPLVM is formulated as the following generative model

$$\begin{aligned} p(\mathbf{Z}) &= \prod_{i=1}^N \mathcal{N}(\mathbf{z}_i|\mathbf{0}, \mathbf{I}) \\ p(\mathbf{F}|\mathbf{Z}, \theta) &= \prod_{j=1}^P \mathcal{N}(\mathbf{f}^{(j)}|\mathbf{0}, \mathbf{K}_{zz}^{(j)}) \\ p(\mathbf{Y}|\mathbf{F}) &= \prod_{j=1}^P p(\mathbf{y}^{(j)}|\mathbf{f}^{(j)}) = \prod_{j=1}^P \prod_{i=1}^N p(y_i^{(j)}|f_i^{(j)}) \end{aligned}$$

In the special case when the emission likelihood is Gaussian, i.e. when $p(\mathbf{y}^{(j)}|\mathbf{f}^{(j)}) = \mathcal{N}(\mathbf{y}^{(j)}|\mathbf{f}^{(j)}, \sigma^2\mathbf{I})$, one can analytically integrate out the GP mappings, resulting in the marginal

$$p(\mathbf{y}^{(j)}|\mathbf{Z}, \theta) = \mathcal{N}(\mathbf{y}^{(j)}|\mathbf{0}, \mathbf{K}_{zz}^{(j)} + \sigma^2\mathbf{I}).$$

Then, inference needs to be carried out on latent variables $\mathbf{z}_1, \dots, \mathbf{z}_N$ and kernel hyperparameters θ only, whereas generally for non-Gaussian emissions we additionally need to infer \mathbf{F} which can no longer be analytically marginalised.

2.3 Scalable inference for Gaussian Processes

Standard inference in GPs scales with $\mathcal{O}(N^3)$ per output dimension, where N is the number of data points. This has motivated the development of low-rank approximations to reduce the computational complexity. One such approach is to introduce M inducing points with $M \ll N$ that lie in the same space as the input data (\mathbf{x} -space for GP regression or \mathbf{z} -space for GPLVM). This effectively reduces the computational complexity to $\mathcal{O}(M^2N)$ - see Quiñero-Candela and Rasmussen [2005] for a review. Titsias [2009] proposed a variational framework where the inducing inputs are treated as variational parameters, allowing us to optimise their

locations by maximising the evidence lower bound (ELBO). This approach was originally proposed for the GP regression model, but has been extended to GPLVM [Titsias and Lawrence, 2010, Damianou et al., 2016], for stochastic variational inference [Hensman et al., 2013], and for non-conjugate likelihoods [Hensman et al., 2015a,b]. Later, a more formal treatment has been provided by Matthews et al. [2016].

Specifically, for the GPLVM, one introduces M inducing input-output pairs, i.e. inputs $\mathbf{Z}_u := (\mathbf{z}_1^u, \dots, \mathbf{z}_M^u)$ and corresponding GP function values $\mathbf{u}^{(j)} = (u_1^{(j)}, \dots, u_M^{(j)})$, where $u_i = f^{(j)}(\mathbf{z}_i^u)$ for each feature $j \in \{1, \dots, P\}$ and inducing point $i \in \{1, \dots, M\}$. In the augmented model now \mathbf{Z}_u become variational parameters, and the joint distribution is assumed to factorize as

$$p(\mathbf{Y}, \mathbf{F}, \mathbf{U}, \mathbf{Z} | \mathbf{Z}_u) = p(\mathbf{Z}) \prod_{j=1}^P p(\mathbf{y}^{(j)} | \mathbf{f}^{(j)}) p(\mathbf{f}^{(j)} | \mathbf{u}^{(j)}, \mathbf{Z}, \mathbf{Z}_u) p(\mathbf{u}^{(j)} | \mathbf{Z}_u),$$

where $p(\mathbf{u}^{(j)} | \mathbf{Z}_u) = \mathcal{N}(\mathbf{u}^{(j)} | \mathbf{0}, \mathbf{K}_{uu})$ is the marginal GP prior over the inducing variables.

3 Covariate-GPLVM

We now consider an extension of the GPLVM to include fixed inputs where we are specifically interested in the *interaction* of the covariates \mathbf{x} and the latent variables \mathbf{z} which we shall call a *covariate-GPLVM*. Specifically, we aim to learn mappings which are defined on the joint space of \mathbf{z} and \mathbf{x} , i.e. $f^{(j)} : (\mathbf{z}, \mathbf{x}) \mapsto \mathbf{y}^{(j)}$. Different assumptions about the form of interaction between \mathbf{z} and \mathbf{x} can be made, and these will correspond to different kernel structures. One approach would be to define the ARD kernel on this joint space:

$$k^{\text{int}}((\mathbf{x}, \mathbf{z}), (\mathbf{x}', \mathbf{z}')) := \sigma_{xz}^2 \exp \left[-\frac{1}{2} \sum_{j=1}^C \left(\frac{x_{ij} - x_{kj}}{l_j^{(x)}} \right)^2 - \frac{1}{2} \sum_{j=1}^Q \left(\frac{z_{ij} - z_{kj}}{l_j^{(z)}} \right)^2 \right].$$

We will initially utilise this general purpose **int** kernel to explore two examples which will motivate our work.

Scalable inducing point based inference (as described in Section 2.3) can be adopted for c-GPLVM in a straightforward way. As the kernels in the c-GPLVM are defined on the extended (product) space of \mathbf{x} and \mathbf{z} so the inducing points now lie in this space which has dimensionality $\dim(\mathbf{x}) + \dim(\mathbf{z})$. Under certain modelling assumptions this dimensionality may be reduced (e.g. when using the additive kernel then we simply need inducing points in the \mathbf{x} and \mathbf{z} space separately and this can reduce the computational cost).

3.1 Pinwheel

First, we consider a synthetic two-dimensional ‘‘pinwheel’’ data as displayed in Figure 4(a). In the observation space, each spoke corresponds to a *trajectory* and we would like to understand the shared properties of how features vary *along* each trajectory irrespective of the *angle* of each spoke. If we had additional, *covariate* information on the clustering structure in the form of these angle (shown by colour coding in Figure 4(a)), we can use this information *jointly* to achieve our goal.

The inferred one-dimensional \mathbf{z} values are shown by colour coding. The standard GPLVM (panel (b)) is unable to uncover the trajectories, whereas the c-GPLVM is able to identify the trajectories within every spoke of the pinwheel (panel (c)). To illustrate what the model has learned, panel (d) shows data generated from the c-GPLVM posterior predictive. Here, the covariate was fixed to the five observed covariate values. Panel (e) explicitly shows the inferred respective GP mappings together with uncertainties (here \mathbf{z} is on x -axis and both features \mathbf{y} are shown on the y -axis, \mathbf{x} was fixed to the five observed values). Panel (f) illustrates the range of GP mappings obtained when interpolating the covariate \mathbf{x} values.

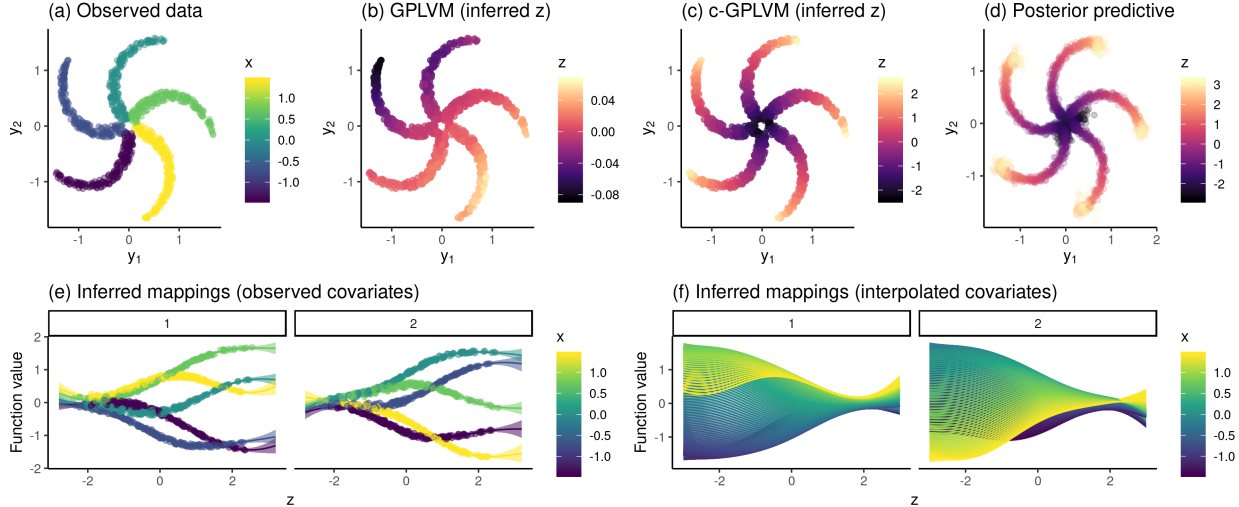


Figure 4: (a) Observed pinwheel shaped two-dimensional data with additional covariate information represented by angle (shown by colour). (b, c) Data points have been coloured according to the inferred \mathbf{z} , using (b) GPLVM, and (c) c-GPLVM. (d) Draws from the c-GPLVM posterior predictive shown in the data space. (e, f) Inferred GP mappings from \mathbf{z} (x -axis) to the observation space (y -axis, \mathbf{y}_1 and \mathbf{y}_2 in two panels respectively). In (e), covariates were fixed to the observed five values, whereas in (f) mappings are shown for a fine grid of covariates.

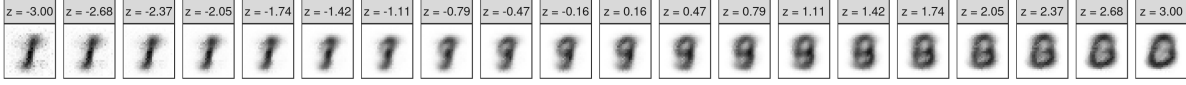
3.2 MNIST hand-written digits

We next consider the MNIST dataset of hand-written digits [LeCun, 1998] as another demonstration of how c-GPLVM can reveal meaningful latent structure that is shared between all 10 digit classes. Here, our expectation is that the shared latent structure will reflect some aspect of handwriting style. Figure 5 illustrates the one-dimensional representations learned by various models: (a) all-class GPLVM, (b) separate GPLVMs for each class and (c) c-GPLVM by showing posterior draws from each model whilst varying \mathbf{z} values in the interval $\mathbf{z} \in [-3, 3]$. Generating from the c-GPLVM is conditional on the class label, so we display results for all ten classes. For GPLVM the single latent dimension does not have a straightforward interpretation as it captures both patterns associated with each digit class as well as shared patterns. The per-class approach (b) does reveal handwriting style but note that these are not aligned across classes. The c-GPLVM can be seen as a unified joint model combining class-specific GPLVMs: now the \mathbf{z} space is shared between all classes. As a result, c-GPLVM has learned to capture handwriting style, underlying all 10 digits, over a continuum: from slanted and less round digits on the left to the opposite on the right.

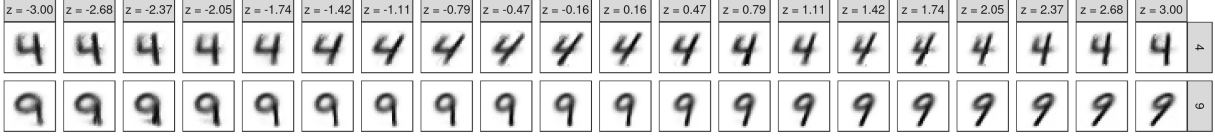
Next we demonstrate the benefits of c-GPLVM for inference in the presence of missing data. In principle, there can be missing values either in some of the features $\mathbf{y}^{(j)}$ or covariates \mathbf{x} . In c-GPLVM, we are able to handle both types of missingness. To demonstrate this on MNIST, we randomly selected 5,000 images and introduced artificial missingness in both. We removed the upper 1/4 corner of the pixels, and compared the predictive performance of c-GPLVM for the imputation of unobserved pixels under two scenarios: missing class labels and known class labels.

As \mathbf{x} is categorical, we implement inference for $\mathbf{x}^{(\text{mis})}$ by introducing the continuous relaxation of the categorical distribution [Maddison et al., 2017] to carry out joint variational inference for c-GPLVM with partially missing inputs. Figure 6 illustrates our experimental setup and displays imputation quality for selected examples (imputation by posterior mean). These were chosen to represent 3 correctly and 3 incorrectly classified data points, to illustrate how missing class labels \mathbf{x} can lead to less accurate imputation in the feature space. The imputation quality for missing pixels has been quantified in Figure 6(d). Most

(a) GPLVM



(b) separate GPLVM for each class



(c) c-GPLVM

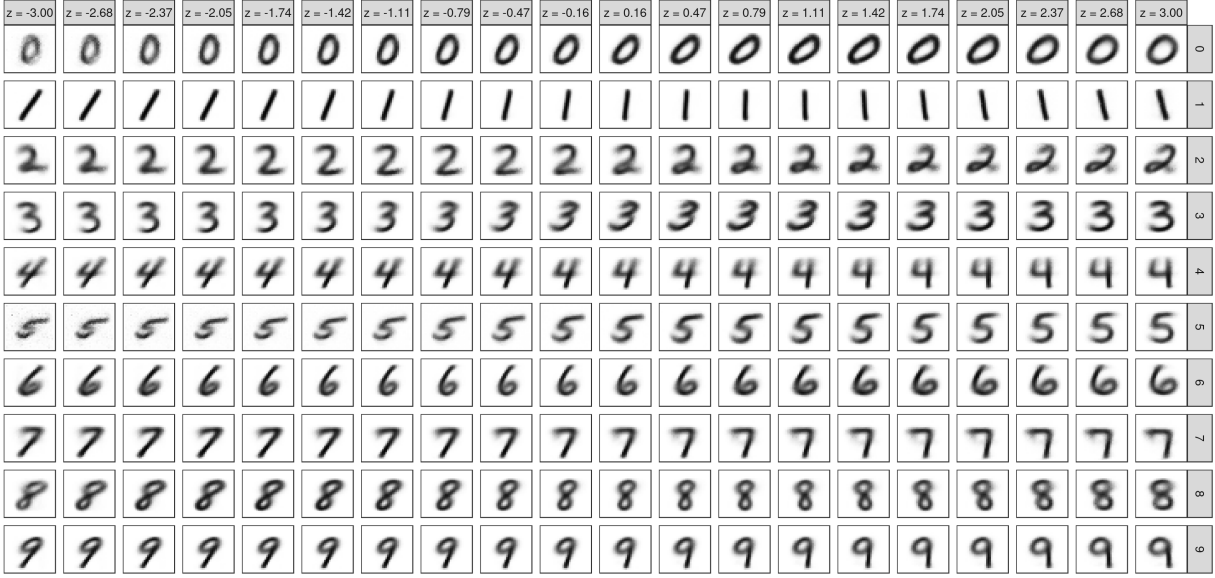


Figure 5: Illustration of the inferred one-dimensional \mathbf{z} for (a) GPLVM, (b) separate GPLVMs for each class (shown for 4 and 9), and (c) c-GPLVM. We generated data from the model when varying \mathbf{z} between -3 and 3 (panels from left to right). For data generation in (b) and (c) we also fixed a class label \mathbf{x} (one-hot-encoding of digits 0 – 9 in rows).

accurate predictions are obtained by c-GPLVM with known \mathbf{x} (average imputation error 0.137), but c-GPLVM with unknown inputs \mathbf{x} is only moderately less accurate (average error 0.147). Both of these provide a higher imputation quality than GPLVM (0.186).

4 Structured c-GPLVM

In predictive applications, as shown in the previous examples, a joint **int** kernel on the fixed and latent inputs may be sufficient to capture a shared latent space across fixed input values. We now turn to consider applications where structured kernels are required in order to promote greater understanding and disentanglement of the effects that are driven by the fixed and/or the latent inputs, both from the latent space perspective as well as how they translate to the observation space.

Our specific motivating example is in modelling disease progression using high-dimensional molecular data (in

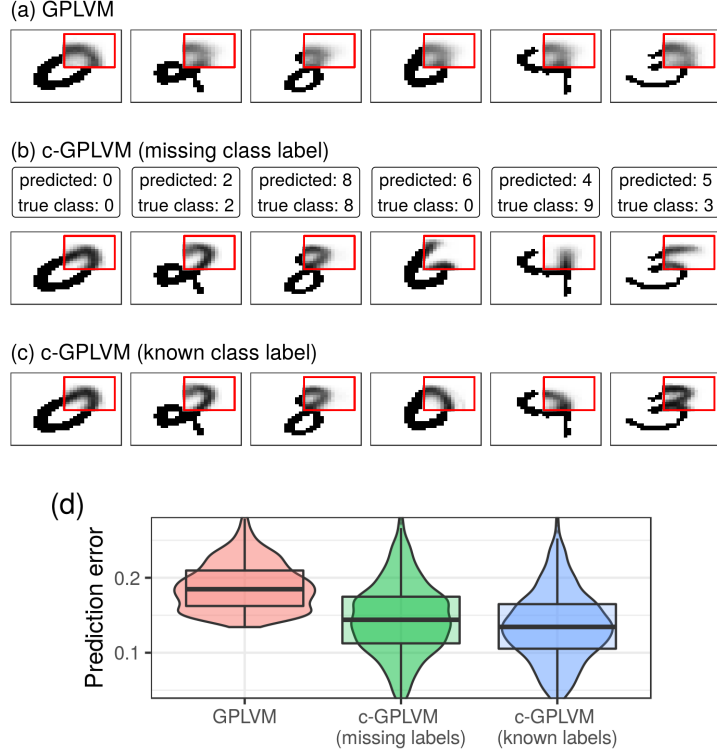


Figure 6: Missing data imputation on MNIST. For 5000 digits the pixel values in the upper corner (red rectangle) were set to be missing. Inferred posterior means shown for six selected examples: (a) GPLVM, (b) c-GPLVM with missing class labels \mathbf{x} , (c) c-GPLVM with known \mathbf{x} . (d) The distribution of mean absolute imputation error over all 5000 data points.

this case RNA sequencing based gene expression analysis). Specifically, consider a number of diseased patients recruited in a cross-sectional study, who are screened at the molecular level (\mathbf{Y}). Each patient will be at a different stage of disease development at the point of recruitment - their molecular data are not *synchronised*. This prevents us from making direct comparisons between patients since, for example, Patient A may have advanced disease and Patient B may have early stage disease. However, these patients essentially have the same disease type and we may postulate that Patient B will eventually evolve to having a molecular state like Patient A at some point in the future. If disease progression (time) is the dominant source of variation, we may imagine that these high-dimensional molecular measurements actually sit on a one-dimensional manifold (\mathbf{z}) where position along the manifold corresponds to a measure of disease progression. Recovering this 1-D manifold is known as the *pseudotime* problem in the genomics literature [Trapnell et al., 2014], where the latent input \mathbf{z} records pseudotime, since it is akin to recovering longitudinal information from a static cross-sectional dataset. Furthermore, each patient may have an additional set of low-dimensional measurements (covariates \mathbf{x}) which may act to modulate their disease progression.

4.1 ADD+INT decomposition

In order to explore these complex relationships between the fixed and latent inputs and observed outputs, we propose a structured c-GPLVM formulation based on mappings of the form

$$f^{(j)}(\mathbf{x}, \mathbf{z}) = f_1^{(j)}(\mathbf{z}) + f_2^{(j)}(\mathbf{x}) + f_3^{(j)}(\mathbf{x}, \mathbf{z})$$

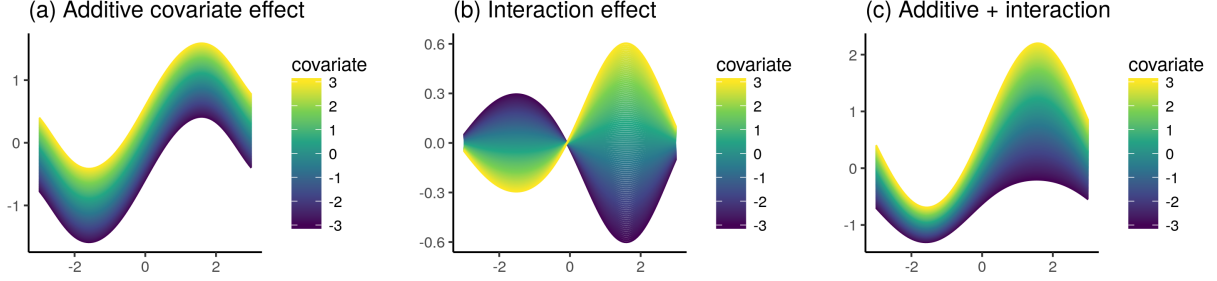


Figure 7: The **add+int** kernel can capture a range of patterns and can identify the presence of (a) additive covariate effect ($\sigma_x^2 > 0$), (b) interaction effect ($\sigma_{xz}^2 > 0$), and (c) a combination of the two ($\sigma_x^2 > 0$, $\sigma_{xz}^2 > 0$). Draws from c-GPLVM for one-dimensional latent \mathbf{z} (on x -axis) and a continuous covariate (colour coding).

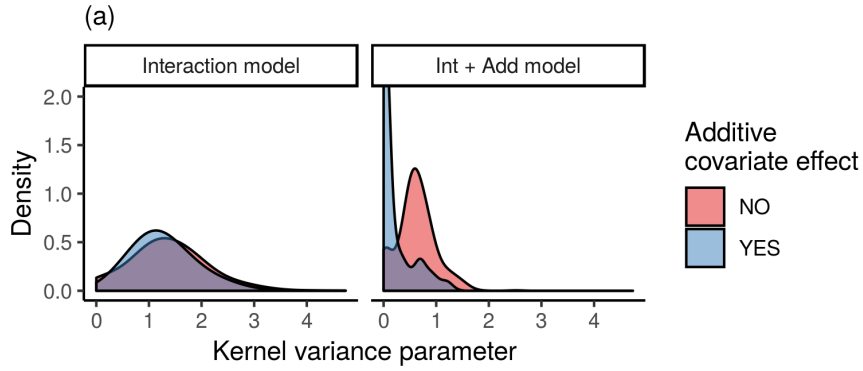


Figure 8: Using the **add+int** kernel decomposition leads to a more interpretable and simple model compared to an **int** (ARD) model. The distribution of σ_{xz}^2 kernel variance for the two models (in two panels). Colour indicates whether an additive component σ_x^2 had a non-zero (blue) or zero (red) contribution in the **add+int** model.

This is a combination of additive and interaction effects. First we define an additive **add** kernel as follows

$$k^{\text{add}}((\mathbf{x}, \mathbf{z}), (\mathbf{x}', \mathbf{z}')) := k^x(\mathbf{x}, \mathbf{x}') + k^z(\mathbf{z}, \mathbf{z}')$$

where both k^x and k^z are squared exponential ARD kernels. Now the above $f^{(j)}(\mathbf{x}, \mathbf{z})$ decomposition corresponds to defining an **add+int** kernel as a sum of two kernels,

$$k^{\text{add+int}}((\mathbf{x}, \mathbf{z}), (\mathbf{x}', \mathbf{z}')) := k^{\text{add}}((\mathbf{x}, \mathbf{z}), (\mathbf{x}', \mathbf{z}')) + k^{\text{int}}((\mathbf{x}, \mathbf{z}), (\mathbf{x}', \mathbf{z}'))$$

To impose identifiability, we make use of Bayesian shrinkage priors on the kernel variances σ_z^2 , σ_x^2 , σ_{xz}^2 so that unnecessary components would be shrunk to zero. This construction allows us to decompose the mapping into additive and interaction components, giving us the ability to interpret how the fixed and latent inputs contribute to feature-level variation. This insight is important because it enables us to understand the molecular features that may drive different aspects of disease progression.

Figure 7 shows example feature-level draws from a structured c-GPLVM with an **add+int** kernel, illustrating the specific behaviours supported. In our disease progression application, we would like to be able to associate each molecular feature with one of these three modes of behaviour.

Fig 8 illustrates the utility of the structured **add+int** kernel. When using simply an ARD kernel on the joint fixed and latent inputs (**int**), all covariate effects (additive or interaction) are absorbed by the ARD model.

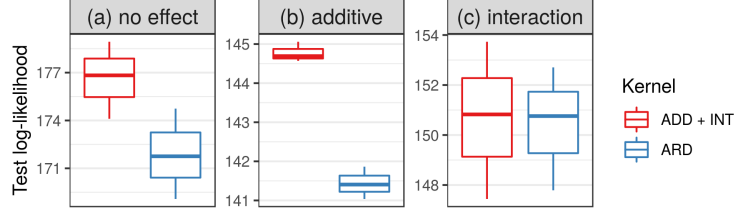


Figure 9: Using **add+int** kernel will result in a higher test log-marginal-likelihoods compared to the standard **int** (ARD) kernel in the scenarios when (a) the covariate is not associated with the features, or when (b) the covariate has an additive effect.

In contrast, an **add+int** kernel decomposition in c-GPLVM is able to identify features with a pure additive component, as demonstrated in a synthetic dataset consisting of a mixture of features with and without additive covariate effects. Furthermore, in scenarios when the true covariate effects are either non-existent or additive, the **add+int** decomposition combined with shrinkage priors provides a means to perform implicit model selection, and as a result, it learns a model with better generalisation compared to than an **int** kernel. This has been illustrated in Figure 9, where we have characterised on synthetic data how well the model generalises to an unseen test set under three scenarios. In the absence of a covariate effect (panel (a)) as well as in the presence of an additive covariate effect (panel (b)), the **add+int** model achieves a higher log-marginal-likelihood on the test set.

4.2 Survival-adjusted disease modelling for TCGA breast cancer data

We now consider a data set consisting of $N = 770$ breast cancers from The Cancer Genome Atlas cohort [Weinstein et al., 2013]. We use gene expression measurements across 500 most variable genes (\mathbf{Y}) and survival information for each patient as a covariate (\mathbf{x}) to explore the relationship between gene expression changes, tumour progression and survival. We modify c-GPLVM to account for *right-censored* survival time covariates in which these inputs have an observed lower bound.

4.2.1 Prediction of survival times

To ensure that our modelling assumptions are aligned with the observed data, we first investigate the survival c-GPLVM in a controlled setting. Specifically we focus on its predictive ability. That is, we consider a subset of individuals whose death times have been observed ($N = 151$) and carry out artificial censoring in batches of size 5. For 5 patients at a time, we artificially censor their survival time by half a year, and fit c-GPLVM to infer the posterior of the true survivals. Results have been shown in Figure 11(c).

We note that *prediction* of survival times is not the primary use case of the c-GPLVM, but it demonstrates the flexibility of the hybrid modelling framework provided by c-GPLVM. When considering alternative methods for the *prediction* of survival times, we note that most models in the field of survival analysis are non- or semi-parametric, i.e. they do not model the baseline hazard function, and thus do not provide a straightforward way for prediction. To obtain a parametric survival model, one common choice is to use the Weibull distribution. Thus, to compare c-GPLVM with a baseline method, we used the Weibull regression model with shrinkage priors as described in [Peltola et al., 2014], predicting patient survival as a function of the gene expression matrix \mathbf{Y} . Figure 10 shows the predictions from the Weibull regression model conditional on patient survival up to the censoring time. In comparison, the predictions made by c-GPLVM are of much higher quality. Note that the c-GPLVM *knows when it does not know*, i.e. the mis-predictions typically have high uncertainty.

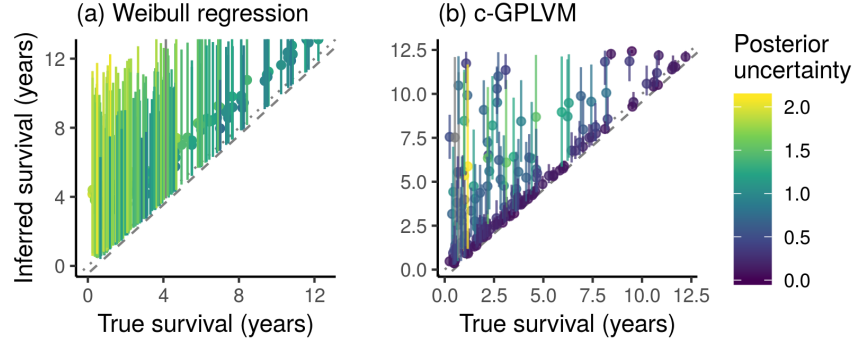


Figure 10: Predicted survival times for artificially censored individuals in TCGA data (true value on x -axis, inferred posterior mean and (5%, 95%) quantiles on y -axis, colour denotes posterior uncertainty) when using (a) Weibull regression model (with predictions made conditional on patient survival up to censoring time), (b) survival c-GPLVM.

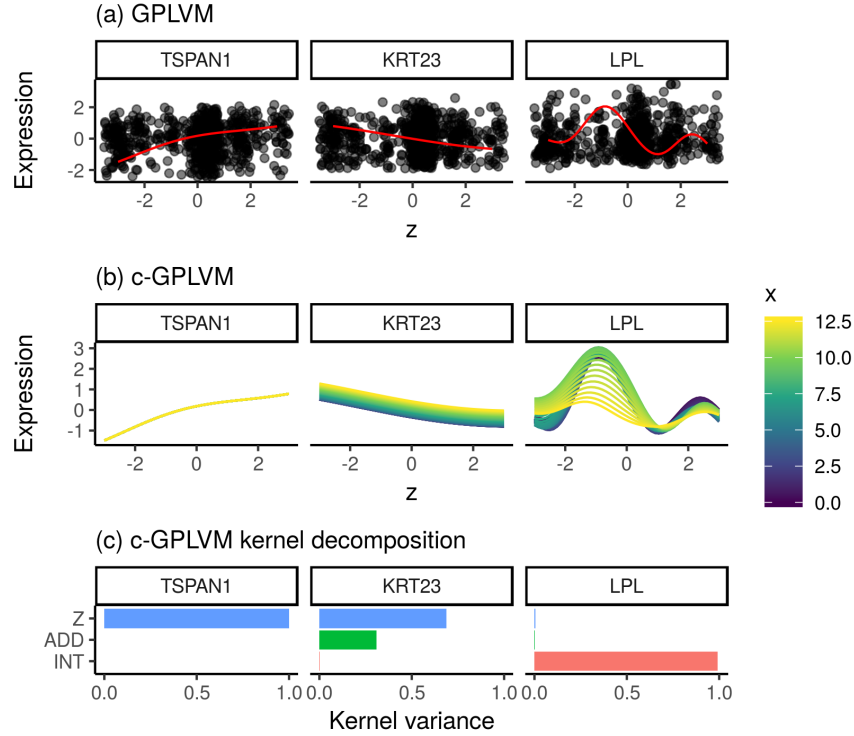


Figure 11: GPLVM (panel A) does not capture the variation driven by the censored covariate (\mathbf{x} =survival), whereas c-GPLVM (panel B) not only captures the effects explained by survival, but in addition, the **add+int** kernel decomposition (panel C) lets us identify three sets of genes: those without any covariate effect (e.g. TSPAN1), genes with an additive covariate effect (e.g. KRT23), and genes that exhibit a complex non-linear interaction (e.g. LPL).

4.2.2 Survival-adjusted cancer modelling

Next, we returned to the original data set of all 770 breast cancers and fitted standard GPLVM and c-GPLVM to the entire cohort. Fig 11a compares a feature-level fit for standard GPLVM and c-GPLVM for three genes *TSPAN1*, *KRT23* and *LPL*. First, *TSPAN1* is a gene that codes for a member of the protein family, Tetraspanins, also known as the transmembrane 4 superfamily. These are small transmembrane glycoproteins which were first described in studies of tumour associated proteins and has been reported to regulate cancer progression in many human cancers [Munkley et al., 2017]. In line with this, structured c-GPLVM identifies *TSPAN1* as a gene whose expression increases along the latent space and not survival. In contrast, Keratin-23 (*KRT23*) decreases with z but is also additively modulated by the survival covariate with patients who survive longer seemingly have higher expression of *KRT23*. Lipoprotein lipase (LPL) plays a role in breaking down fat in the form of triglycerides, which are carried from various organs to the blood by molecules called lipoproteins. This gene is identified as having interaction effects and we see that there is a range of latent input values $-2 < z < 0$ where low LPL expression is associated with longer survival and high LPL expression is associated with reduced lifespan. This suggests that during certain periods of breast cancer development, high levels of LPL activity could enable aggressive disease progression possibly through acting to provide a supply of fatty acids to fuel tumour growth [Kuemmerle et al., 2011].

5 Related Work

Hybrid latent variable models, i.e. models which map (\mathbf{z}, \mathbf{x}) to the observation space, have been previously developed in other domains. For example, Campbell and Yau [2018] consider a covariate-adjusted *linear* latent variable model which can be seen as an extension of factor analysis. Similarly, in the deep learning domain, conditional VAEs [Kingma et al., 2014, Sohn et al., 2015] can be thought of as covariate-adjusted VAEs. Our c-GPLVM extends GPLVMs in a similar way.

Regarding GP-based hybrid models, a number of alternative approaches have been developed which can be said to lie on the spectrum between GPR and GPLVMs. Latent GP regression models (LGPR) [Wang and Neal, 2012, Bodin et al., 2017] extend the input space of a GP regression model with additional latent variables that are used to modulate the covariance function. Approximate marginalisation of the latent variables allows these models to consider non-stationary, multimodal behaviour. LGPR models often implicitly assume that the dimensionality of the latent variables is less than the number of regressors $\dim(\mathbf{x}_n) \gg \dim(\mathbf{z}_n)$. In this sense, LGPR is closer to a GP regression model compared to a GPLVM. Thus it can be seen as an extension of the former, with the addition of the latent variables which provide flexibility to characterise *unknown* sources of variability. Note that this is different from c-GPLVM which aims to capture the extra variability from *known* covariates, and which can be seen as an extension of the GPLVM. Semi-described and semi-supervised learning in GP regression is considered by [Damianou and Lawrence, 2015] when the inputs (or outputs) are partially observed or uncertain, this formulation also leads to a hybrid model with latent variables introduced in place of missing data.

Supervised GPLVM encompass a family of related ideas seek to decompose the joint distribution $p(\mathbf{y}, \mathbf{x}, \mathbf{z})$ in different ways. For example, in [Gadd et al., 2018], the joint distribution is factorised such that the latent variables are conditionally dependent on the covariates $p(\mathbf{z}|\mathbf{x})$. Whilst in the supervised-GPLVM formulation [Gao et al., 2011] and the shared-GPLVM [Shon et al., 2006] both observations and fixed inputs are conditionally dependent on the latent inputs, $p(\mathbf{y}|\mathbf{z})p(\mathbf{x}|\mathbf{z})$. In the discriminative-GPLVM [Urtasun and Darrell, 2007], class label information is used to maximise the discriminatory power between discrete classes in the latent space by placing a prior on the latent positions $p(\mathbf{z})$ which corresponds to a measure of between-class separability to within-class variability. This is fundamentally different from c-GPLVM which learns a *covariate-adjusted* \mathbf{z} , as illustrated in Figures 2 and 3.

The Automatic Statistician [Duvenaud et al., 2013] performs searches for optimal combinations of kernels in

GP models. In c-GPLVM we introduced a fixed but structured kernel allowing decomposition of the observed heterogeneity into additive and interaction components using sparse priors for which no model search was required.

6 Discussion

We have introduced a covariate-GPLVM that integrates GP regression and latent variable modelling with a specific focus on the interaction between covariates and latent variables. The c-GPLVM learns latent spaces that reveal structure in the data which is shared across covariate values. By making use of GP mappings that are specified on the extended joint space of covariates and latent variables, we can model complex non-linear dependencies, while maintaining interpretable and decomposable mappings.

The c-GPLVM is applicable for a wide range of applications where there is known structure accounting for variance attributable to this structure. This encompasses scenarios when we are interested in explicitly exploring the interactions between this covariate information and other features, as well as those where such covariates are “nuisance” variables and we would like to adjust for confounding factors (e.g. batch effects or the presence of different ancestral populations in population genetics).

Acknowledgements

KM is supported by a UK Engineering and Physical Sciences Research Council Doctoral Studentship. KRC is supported by a Banting postdoctoral fellowship from the Canadian Institutes of Health Research, and postdoctoral fellowships from the Canadian Statistical Sciences Institute and the UBC Data Science Institute. CY is supported by a UK Medical Research Council Research Grant (Ref: MR/P02646X/1).

References

- Erik Bodin, Neill DF Campbell, and Carl Henrik Ek. Latent gaussian process regression. *arXiv preprint arXiv:1707.05534*, 2017.
- Kieran R Campbell and Christopher Yau. Uncovering pseudotemporal trajectories with covariates from single cell and bulk expression data. *Nature Communications*, 9(1):2442, 2018.
- Andreas Damianou and Neil D Lawrence. Semi-described and semi-supervised learning with gaussian processes. *31st Conference on Uncertainty in Artificial Intelligence (UAI)*, 2015.
- Andreas C Damianou, Michalis K Titsias, and Neil D Lawrence. Variational inference for latent variables and uncertain inputs in gaussian processes. *The Journal of Machine Learning Research*, 17(1):1425–1486, 2016.
- David Duvenaud, James Robert Lloyd, Roger Grosse, Joshua B Tenenbaum, and Zoubin Ghahramani. Structure discovery in nonparametric regression through compositional kernel search. *arXiv preprint arXiv:1302.4922*, 2013.
- Charles Gadd, Sara Wade, Akeel Shah, and Dimitris Grammatopoulos. Pseudo-marginal bayesian inference for supervised gaussian process latent variable models. *arXiv preprint arXiv:1803.10746*, 2018.
- Xinbo Gao, Xiumei Wang, Dacheng Tao, and Xuelong Li. Supervised gaussian process latent variable model for dimensionality reduction. *IEEE Transactions on Systems, Man, and Cybernetics, Part B (Cybernetics)*, 41(2):425–434, 2011.
- James Hensman, Nicolo Fusi, and Neil D Lawrence. Gaussian processes for big data. *Uncertainty in Artificial Intelligence*, 2013.

- James Hensman, Alexander G Matthews, Maurizio Filippone, and Zoubin Ghahramani. MCMC for variationally sparse gaussian processes. In *Advances in Neural Information Processing Systems*, pages 1648–1656, 2015a.
- James Hensman, Alexander G de G Matthews, and Zoubin Ghahramani. Scalable variational gaussian process classification. 2015b.
- Diederik P Kingma and Max Welling. Auto-encoding variational bayes. *Proceedings of the International Conference on Learning Representations (ICLR)*, 2014.
- Diederik P Kingma, Shakir Mohamed, Danilo Jimenez Rezende, and Max Welling. Semi-supervised learning with deep generative models. In *Advances in Neural Information Processing Systems*, pages 3581–3589, 2014.
- Nancy B Kuemmerle, Evelien Rysman, Portia S Lombardo, Alison J Flanagan, Brea C Lipe, Wendy A Wells, Jason R Pettus, Heather M Froehlich, Vincent A Memoli, Peter M Morganelli, et al. Lipoprotein lipase links dietary fat to solid tumor cell proliferation. *Molecular cancer therapeutics*, pages molcanther-0802, 2011.
- Matt J Kusner, Brooks Paige, and José Miguel Hernández-Lobato. Grammar variational autoencoder. *arXiv preprint arXiv:1703.01925*, 2017.
- Neil Lawrence. Probabilistic non-linear principal component analysis with gaussian process latent variable models. *Journal of machine learning research*, 6(Nov):1783–1816, 2005.
- Yann LeCun. The mnist database of handwritten digits. <http://yann.lecun.com/exdb/mnist/>, 1998.
- Laurens van der Maaten and Geoffrey Hinton. Visualizing data using t-sne. *Journal of machine learning research*, 9(Nov):2579–2605, 2008.
- Chris J Maddison, Andriy Mnih, and Yee Whye Teh. The concrete distribution: A continuous relaxation of discrete random variables. *International Conference on Learning Representations*, 2017.
- Alexander G de G Matthews, James Hensman, Richard Turner, and Zoubin Ghahramani. On sparse variational methods and the kullback-leibler divergence between stochastic processes. In *Artificial Intelligence and Statistics*, pages 231–239, 2016.
- Jennifer Munkley, Urszula L McClurg, Karen E Livermore, Ingrid Ehrmann, Bridget Knight, Paul McCullagh, John McGrath, Malcolm Crundwell, Lorna W Harries, Hing Y Leung, et al. The cancer-associated cell migration protein tspan1 is under control of androgens and its upregulation increases prostate cancer cell migration. *Scientific reports*, 7(1):5249, 2017.
- Tomi Peltola, Aki S Havulinna, Veikko Salomaa, and Aki Vehtari. Hierarchical bayesian survival analysis and projective covariate selection in cardiovascular event risk prediction. In *Proceedings of the Eleventh UAI Conference on Bayesian Modeling Applications Workshop-Volume 1218*, pages 79–88. Citeseer, 2014.
- Joaquin Quiñonero-Candela and Carl Edward Rasmussen. A unifying view of sparse approximate gaussian process regression. *Journal of Machine Learning Research*, 6(Dec):1939–1959, 2005.
- Carl Edward Rasmussen and Christopher KI Williams. *Gaussian process for machine learning*. MIT press, 2006.
- Aaron Shon, Keith Grochow, Aaron Hertzmann, and Rajesh P Rao. Learning shared latent structure for image synthesis and robotic imitation. In *Advances in neural information processing systems*, pages 1233–1240, 2006.
- Kihyuk Sohn, Honglak Lee, and Xinchen Yan. Learning structured output representation using deep conditional generative models. In *Advances in Neural Information Processing Systems*, pages 3483–3491, 2015.

- Casper Kaae Sønderby, Tapani Raiko, Lars Maaløe, Søren Kaae Sønderby, and Ole Winther. Ladder variational autoencoders. In *Advances in neural information processing systems*, pages 3738–3746, 2016.
- Michael E Tipping and Christopher M Bishop. Probabilistic principal component analysis. *Journal of the Royal Statistical Society: Series B (Statistical Methodology)*, 61(3):611–622, 1999.
- Michalis Titsias. Variational learning of inducing variables in sparse gaussian processes. In *Artificial Intelligence and Statistics*, pages 567–574, 2009.
- Michalis Titsias and Neil D Lawrence. Bayesian gaussian process latent variable model. In *Proceedings of the Thirteenth International Conference on Artificial Intelligence and Statistics*, pages 844–851, 2010.
- Cole Trapnell, Davide Cacchiarelli, Jonna Grimsby, Prapti Pokharel, Shuqiang Li, Michael Morse, Niall J Lennon, Kenneth J Livak, Tarjei S Mikkelsen, and John L Rinn. The dynamics and regulators of cell fate decisions are revealed by pseudotemporal ordering of single cells. *Nature biotechnology*, 32(4):381, 2014.
- Raquel Urtasun and Trevor Darrell. Discriminative gaussian process latent variable model for classification. In *Proceedings of the 24th international conference on Machine learning*, pages 927–934. ACM, 2007.
- Chunyi Wang and Radford M Neal. Gaussian process regression with heteroscedastic or non-gaussian residuals. *arXiv preprint arXiv:1212.6246*, 2012.
- John N Weinstein, Eric A Collisson, Gordon B Mills, Kenna R Mills Shaw, Brad A Ozenberger, Kyle Ellrott, Ilya Shmulevich, Chris Sander, Joshua M Stuart, Cancer Genome Atlas Research Network, et al. The cancer genome atlas pan-cancer analysis project. *Nature genetics*, 45(10):1113, 2013.